

# Segmentation of Tuberculosis Bacilli Using Watershed Transformation and Fuzzy C-Means

Rahadian Kurniawan<sup>1</sup>, Izzati Muhimmah<sup>2</sup>, Arrie Kurniawardhani<sup>3</sup>, and Sri Kusumadewi<sup>4</sup>  
<sup>1–4</sup>Department of Informatics, Faculty of Industrial Technology, Universitas Islam Indonesia  
Yogyakarta 55584, Indonesia

Email: <sup>1</sup>rahadiankurniawan@uii.ac.id, <sup>2</sup>izzati@uii.ac.id, <sup>3</sup>arrie.kurniawardhani@uii.ac.id,  
<sup>4</sup>sri.kusumadewi@uii.ac.id

**Abstract**—The easily transmitted Tuberculosis (TB) disease is attributed to the fact that Mycobacterium Tuberculosis (MTB) bacteria/viruses can be transmitted through the air. One of the methods to screen the TB disease is by reading sputum slides. Sputum slides are colored sputum samples of TB patients placed on microscopic slides. However, TB disease microscopic analysis has some limitations since it requires high accuracy reading and well-trained health personnel to avoid errors in the process of interpretation. Furthermore, the number of TB patients in the Primary Health Care (PHC) and the process of manual calculation of bacteria in a field of view often complicate the decision-making in the screening process conducted by the medical staffs. In this paper, the researchers propose the use of Watershed Transformation and Fuzzy C-Means combination to help solve the problem. The researchers collect the photo shooting of three PHC in Indonesia with 55 images of sputum from different TB patients. The assessed results of the proposed method are compared with the opinions of three Microbiology doctors. The comparison shows Cohen's Kappa Coefficient value of 0.838. It suggests that the proposed method can detect Acid Resistant Bacteria (ARB) although it needs some improvement to achieve higher accuracy.

**Index Terms**—Tuberculosis, Segmentation, Mycobacterium Tuberculosis, Fuzzy C-means, Watershed Transformation

## I. INTRODUCTION

**T**UBERCULOSIS (TB), one of the deadliest diseases in the world, is a highly contagious disease caused by Mycobacterium Tuberculosis (MTB). The TB disease is transmitted very easily through the air. It was estimated globally that 10 million people developed TB disease in 2017. Unfortunately, Indonesia ranks third as the world's largest TB patient [1]. In order to address the high number of TB patients in Indonesia, the early detection of TB disease is urgently

needed in the level of Primary Health Care (PHC) like in public health care 'Puskesmas'. TB treatment is not successful if the doctor's actions and prescriptions are inaccurate, the quality of the drug is poor due to delivery problems, and drug intake is insufficient [2]. It is necessary for patients to get early treatment because the appropriate patient's handling can reduce the clinical worsening of TB [3].

Based on the Decree of Minister of Health of the Republic of Indonesia no. 364/MENKES/SK/V/2009 [4], TB diagnosis can be done by microscopically sputum examination. TB patients' sputum examinations are performed with a bright-field microscope technique in most PHCs in Indonesia. There are many methods for detecting the TB disease such as the Tuberculin Skin Test (TST), Chest X-ray, Interferon-Gamma Release Assay (IGRA), Culture Test, and GeneXpert. However, microscopic sputum smear examination is a widely used technique and also provides faster results compared to other tests [5]. To facilitate the observation, the sputum image is stained with the Ziehl-Neelsen (ZN) smear method. The ZN staining method is one of the techniques commonly used to diagnose TB infection.

Clinically, sputum slide preparation is manually checked by a pathologist through a microscope. This certainly poses some challenges such as long and tiring reading times, and it definitely requires expertise [6] since the used data should show 100 field views of a sputum preparation. If only one field is open, there is a possibility that MTBs are available in the other field of view. In addition, the lack of well-trained medical personnel in the process of sputum slide staining in PHC leads to poor staining process and produces complex images for interpretation. Furthermore, the number of TB patients in the PHC and the manual counting of bacteria in a field of view often complicate medical

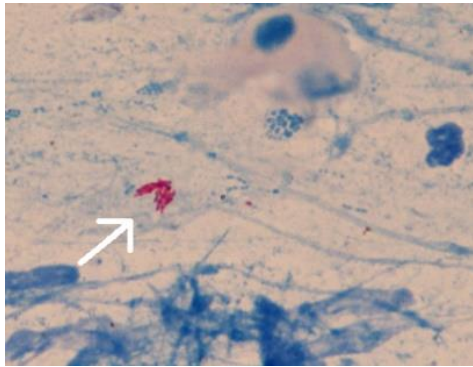


Fig. 1. Sputum image with overlapping acid resistant bacteria (as shown by the arrow).

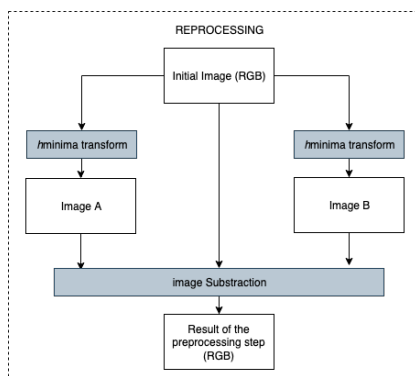


Fig. 2. Schematic of the preprocessing step.

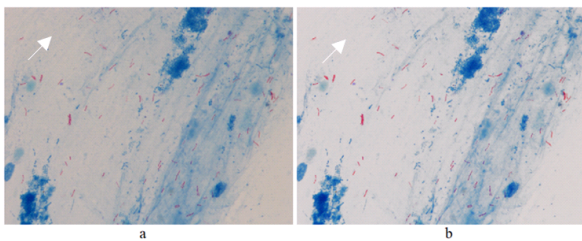


Fig. 3. (a) Original image, (b) Image of preprocessing stage. Figure 3b shows a better contrast in the background and acid resistant bacteria than 3a.

personnel in giving medical decisions. As reported by Ref. [7], the decision by experts occasionally is mistrusted because it is subjective, emotional, and recorrected when misdiagnosis happens.

The patient’s sputum screening process with ZN can help medical personnel to identify microscopic MTBs characterized by red spots on the image. Red spots indicate the presence of Acid Resistant Bacteria (ARB) in a sputum image. The interviews with three Microbiology doctors reveal that to determine whether the spots on the sputum image can be classified as MTB or not requires the culture test. However, the

Culture Test needs early screening done by identifying the presence of ARB and knowing its number. Figure 1 illustrates the existence of ARB in a sputum image.

There have been several studies addressing the MTB identification domain on the sputum image automatically to help pathologists increasing the speed and accuracy of TB disease diagnosis. The MTB identification process in the sputum image automatically includes several phases, namely: image quality improvement, segmentation, feature extraction, and classification/identification. Some techniques are proposed to improve image quality such as Adaptive Color Thresholding [8], linear stretching in Red-Green-Blue (RGB) or Hue-Intensity-Saturation (HIS) color space [9]. A good quality sputum image can improve the success of the segmentation process. Some used techniques for the MTB segmentation process include  $k$ -means clustering [8, 10–12], Self-Organizing Map [13], Watershed Transformation [14], and Adaptive Signal Processing [15]. The color characteristics of MTB tend to differ from the background. Therefore, color is used as a reference in a grouping with the  $k$ -means clustering method. Some of the trials to identify the color space is the Commission Internationale de l’Eclairage Lab (CIELAB) [8], RGB [10], and HSI [16]. Although some previous researchers have investigated this matter, they have not targeted the specific Indonesian image data that sputum images taken from PHC have lesser intensity and contrast, contain noise, and have low resolution.

This research intends to propose a new method to detect and calculate the presence of ARB automatically through sputum microscopic images accurately. Then, the result will be compared to the results of manual readings by three Microbiology doctors. This research uses the data of specific sputum image of Indonesian people obtained from PHC. Furthermore, this research is expected to help health workers especially physicians to detect ARB faster and assist them in giving medical decisions. In addition, the proposed method may reduce the involvement of health personnel in the TB screening process in the laboratory as a decision support tool. The research is the first step to finding the right method for identifying MTBs.

## II. RESEARCH METHOD

### A. Preprocessing

The used sputum image data suffers a poor contrast. To get the candidate position of ARB, the researcher needs to find the red color on the image. The red color in the sputum image that has been given ZN coloration indicates the presence of ARB. The preprocessing step is summarized in Fig. 2.

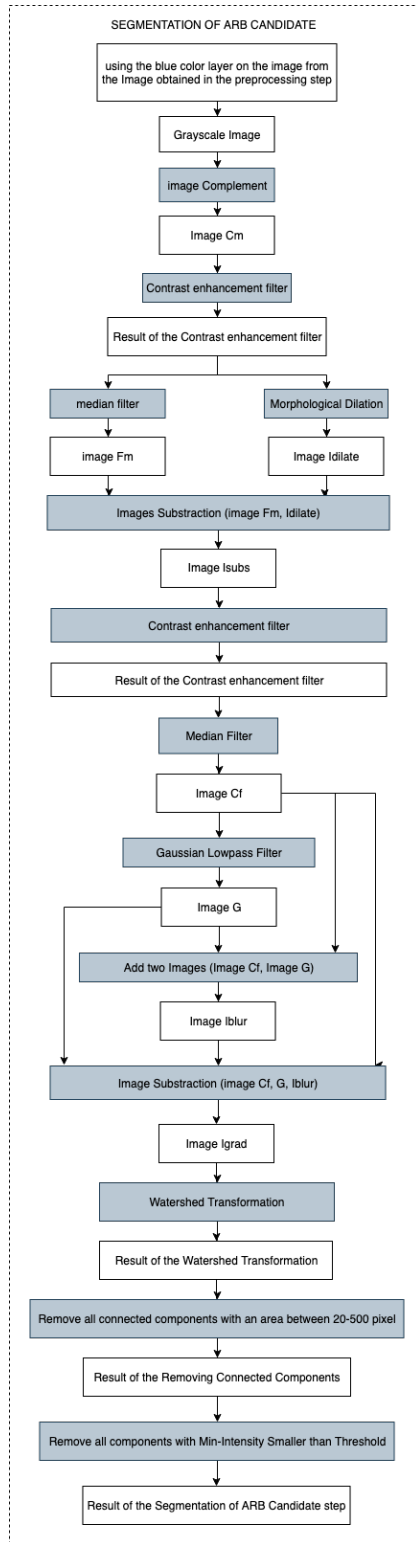


Fig. 4. Schematic of acid resistant bacteria candidate segmentation.

At the first stage, the researchers need to increase the intensity of red in the image. The first stage is

the preprocessing. It is done by applying the  $h$ -minima transform [17] to the original image ( $I$  image) on each layer of color (red ( $r$ ), green ( $g$ ), blue ( $b$ )) with the value of  $h$  in each layer of color obtained through the following equations:

$$h_r = \frac{\mu(I_r)}{2}, \quad (1)$$

$$h_g = \frac{\mu(I_g)}{2}, \text{ and} \quad (2)$$

$$h_b = \frac{\mu(I_b)}{2} \quad (3)$$

where  $\mu$  is a mean of intensity value in one of the color channel of  $I$  image;  $h_r$ ,  $h_g$ , and  $h_b$  is the  $h$  value used in  $h$ -minima transform. After the image output is generated through the transformation process, it is named after  $A$  image.

On the other hand, the  $B$  image is obtained by  $h$ -minima transformation of the original image ( $I$  image) with the lowest non-zero value of each color layer. The preprocessing stage is terminated by subtracting the  $I$  image with the result of subtraction of  $A$  and  $B$  images as follows:

$$P(x, y) = I(x, y) - A(x, y) - B(x, y). \quad (4)$$

The operation of subtracting the intensity value per layer of the original image color with an average value followed by the minimum value will make the high color intensity dominant. When the three layers are combined, it yields a sharp color intensity. This process gives better contrast images as seen in Fig. 3. Figure 3b shows that the color contrast has been improved from the original images.

### B. Segmentation of ARB Candidate

The next step is to segment the areas containing ARB. At this stage, grayscale images are used from the preprocessing stage using the blue color layer on the image. A series of segmentation trials using single layer values (singular red, singular blue, and singular green and gray) seems to obtain the best result on a singular blue color layer. This singular layer approach on the segmentation process has benefit in term of computational load that leads to reducing computation time. This finding is also reported by Ref. [18] as the best color contrast to detect ARB. The segmentation of ARB Candidate step is summarized in Fig. 4.

The first step in ARB candidate segmentation is to perform the complement process to the image of the preprocessing stage in the blue layer. This complement image refers to as  $C_m$  image. Furthermore, the contrast enhancement of the filter process is done on  $C_m$  image to sharpen the contrast with 1% of

saturates at low intensity and 1% at high intensity. The resulted image of the contrast enhancement filter process is carried out by the median filtering process to smooth the image texture. Further morphological dilation is performed on the image produced in the median filtering process using a flat square Structuring Element ( $SE$ ) with a radius of 8 as followings:

$$I_{dilate} = F_m \oplus SE \quad (5)$$

where  $\oplus$  is the dilation operator, and  $F_m$  is the image resulted from the median filtering process.

Furthermore, gradient morphology is done by subtracting between the morphological process resulted in dilation with the median resulted from median filtering. It uses Eq. (6) as follows:

$$I_{subs} = (I_{dilate} - f_m). \quad (6)$$

The next contrast enhancement filters are performed on  $I_{subs}$  image to sharpen the contrast with 1% saturates at low intensity and 1% at high intensity. The image resulted from the contrast enhancement filter process is reprocessed with the median filtering to smooth the image texture. The image resulted from the median filtering process refers to  $C_f$  image. The  $C_f$  image is processed with Gaussian Lowpass filter with the kernel equation as follows:

$$kernel = [4 \times \sigma + 1, \sigma] \quad (7)$$

where the used  $\sigma$  (standard deviation) is 10. The used  $\sigma$  value in this research is from a series of test on the used datasets. The image of Gaussian Lowpass filter process refers to  $G$  image. Afterward, the researchers conduct the process of adding up the image which is generated from the Gaussian Lowpass filter process with the median filtering process as follows:

$$I_{blur} = (G + Cf) \quad (8)$$

where  $Cf$  is the resultant of median filtering (see Fig. 3). Subsequently, the researchers conduct the image subtraction process to perform the gradient morphology process through Eq. (10).

$$I_{grad} = Cf - (I_{blur} - I_{dilate}) \quad (9)$$

The results of gradient morphological processes can be seen in Fig. 5b. Based on the gradient morphological image ( $I_{grad}$ ), the researchers perform the Watershed Transformation process [19] to obtain the ARB candidate segmentation. The results of the Watershed Transformation process can be seen in Fig. 6b. This Watershed Transformation results in a large number of areas that are the candidate segments of ARB. Therefore, it is necessary to reduce or filter the result of the segmentation to help to improve the performance

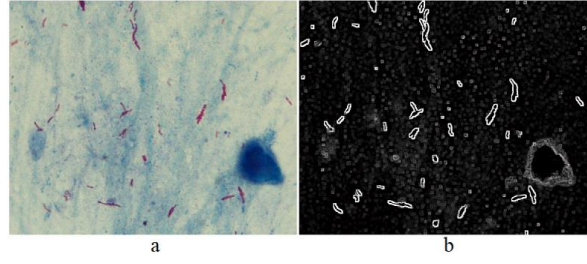


Fig. 5. (a) Original image, (b) Gradient morphological image.

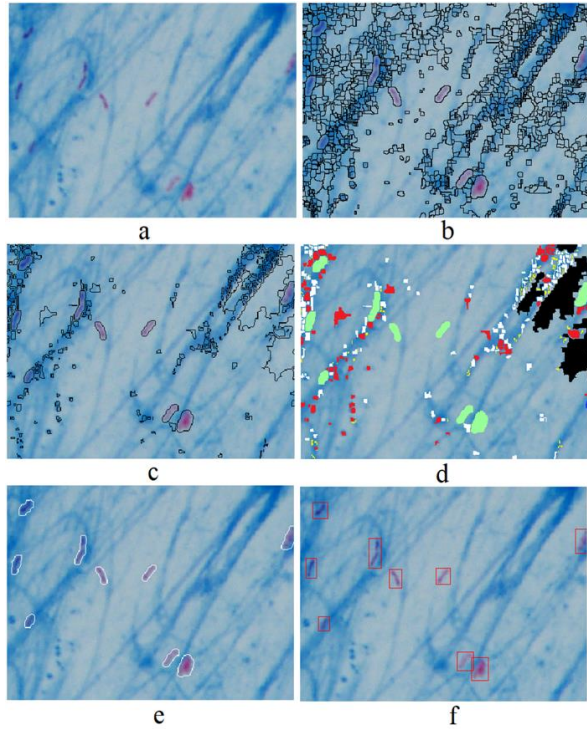


Fig. 6. (a) Original image, (b) Watershed Transformation segmentation image, (c) Watershed Transformation imagery subtracted by the number of existing labels based on the minimal color of each label, (d) FCM Clustering result image using five classes, (e) Class resulted from clustering process, (f) Original image with red box marker indicating location of Acid Resistant Bacteria.

of the next clustering. The reduction of the resulted ARB candidate area is done by looking for segmentation results with more than 20 pixels but less than 500 pixels area [20]. The reduced segmentation results are reduced again using the minimum color intensity criterion at the blue layer. The area with minimal color intensity on the color layer which is smaller than the threshold value will be maintained. However, if it is greater than the threshold value, it will be discarded. The value of the threshold used in the research is derived from the following equation:

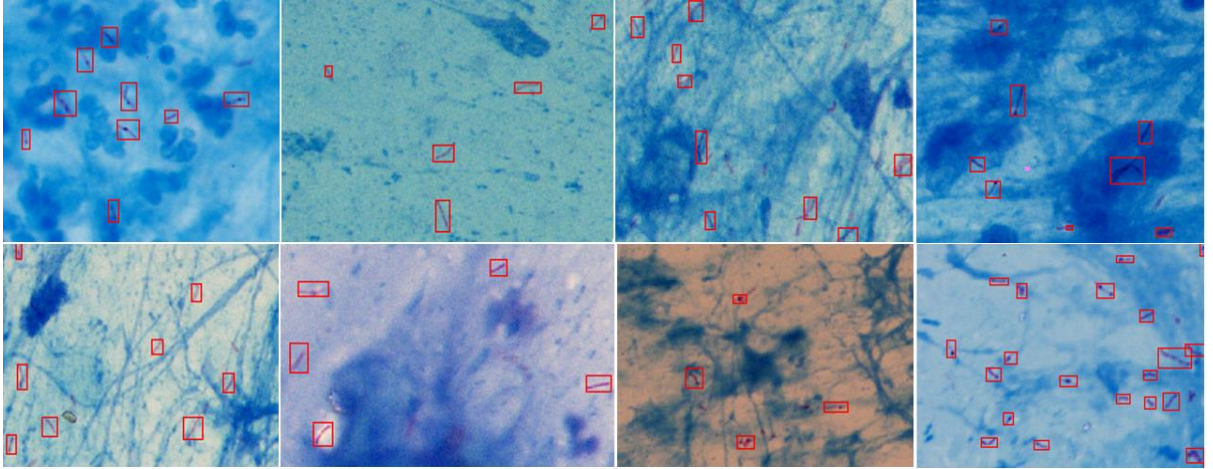


Fig. 7. The result of the proposed method in some sputum images.

$$\text{Threshold} = \mu(I_b) - \sigma(I_r) \quad (10)$$

where  $\mu(I_b)$  is the average value of the true color of the original image in the blue color layer, and  $\sigma(I_r)$  is the standard deviation of the intensity of the original image color in the red color layer. The result of the reduction of ARB candidate area with this color intensity can be seen in Fig. 6c.

### C. Clustering

The final step of this process is clustering. Before carrying out the clustering process, the researchers apply a feature extraction process from the ARB segmentation result. Feature extraction is performed by using four features referring to Refs. [11, 20, 21]. Those are perimeter, area, eccentricity, and the maximum intensity value of each ARB candidate. The perimeter is the number of pixels in the ARB candidate boundary area. Then, area refers to the area of ARB candidate segmentation, while the maximum value is obtained from the highest value in each ARB candidate area in the original Image grayscale image. Moreover, eccentricity is the degree of the burden of an object. Eccentricity is derived from the following equation:

$$e = \frac{\sqrt{\text{semi\_major axis}^2 - \text{Semi\_minor axis}^2}}{\text{semi\_major axis}}. \quad (11)$$

The next Fuzzy C-Means clustering is to divide the previously found area. Fuzzy C-Means clustering is used because this method results in a high level of accuracy in the previous research by Ref. [22]. This research uses five numbers of classes. These numbers of classes are selected from a series of tests resulting in the number of five for the class as the most

precise cluster value [18]. The results of each stage of clustering can be seen in Figs. 6d and 6e.

In Fig. 6d, the image of ARB candidate segmentation has been split into five classes. The color distinguishes each class. Furthermore, a set of clusters containing ARB is further separated like in Fig. 6e. Figure 6e shows that the proposed algorithm can recognize ARB in the sputum image.

## III. RESULTS AND DISCUSSION

### A. Data

The used images are from the photo shooting of three PHCs in Indonesia with 55 sputum images from different TB patients using the Olympus DP20 Microscope with 100x magnification. The images are saved in JPEG format with  $1600 \times 1200$  pixels. These images have been verifying by tree Microbiology doctors and are considered feasible for the interpretation process.

### B. Evaluation

#### 1) Computational Time Testing.

Table I illustrates the computational time at each step. It is to test the efficiency level of the proposed method built using the MATLAB software with the Pentium 2.66 GHz computer and 4 GB RAM. It also pinpoints that the average processing time per image is  $\pm 13.21$  seconds.

#### 2) System Performance.

At this stage, the researchers compare the results of the proposed detection method with the manual reading by Expert (expert truth). It is noteworthy that out of 55 sputum images used, the three Microbiology doctors successfully approve only

TABLE I  
COMPUTATIONAL TIME.

Steps	Time (sec) mean $\pm$ std
Preprocessing	0.25 $\pm$ 0.02
ARB Candidate Segmentation	11.59 $\pm$ 4.40
Clustering	1.37 $\pm$ 0.17

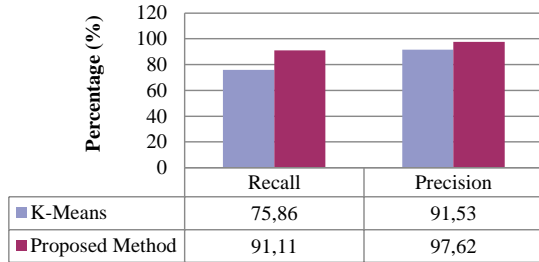


Fig. 8. Results of the application of the proposed method and  $k$ -means clustering for precision and recall.

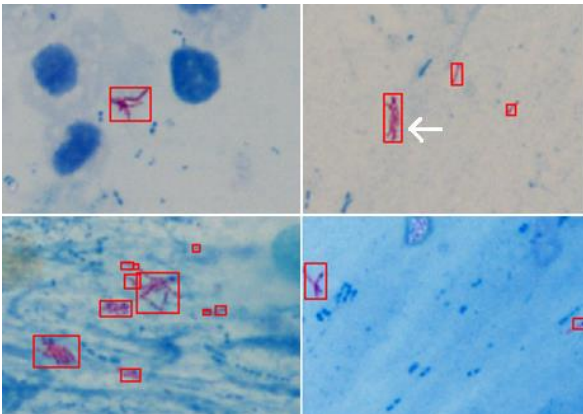


Fig. 9. The result of ARB segmentation does not break the overlapping Acid Resistant Bacteria.

47 images. Therefore, there are only 47 images to be compared to the results of the interpretation at this stage. The test is conducted using Cohen's Kappa Coefficient. The value of the agreement intensity between the results of a manual test by the expert with the proposed method resulted uses Eq. (12):

$$k = \frac{Pr(a) - Pr(e)}{1 - Pr(e)}, \quad (12)$$

it shows that  $Pr(a)$  is the relative observed agreement among raters, and  $Pr(e)$  is the hypothetical probability of chance agreement. Based on the agreement with three Microbiology doctors, the proposed method is divided to three classes (ARB>10 is for images with more than 10 ARBs,

TABLE II  
RESULTS OF SYSTEM COMPARISON AND EXPERT EVALUATION.

		Proposed Method			Total
		ARB>10	ARB<10	ARB=0	
Manual	ARB > 10	21	4	0	25
	ARB < 10	1	17	0	18
	ARB = 0	0	0	4	4
	Total	22	21	4	47

TABLE III  
RESULTS OF SYSTEM COMPARISON AND EXPERT EVALUATION.

Kappa Value	Agreement Intensity
0.00 – 0.20	Very Low
0.21 – 0.40	Low
0.41 – 0.60	Enough
0.61 – 0.80	Strong
0.81 – 1.00	Very Strong

ARB<10 for images with less than 10 ARBs, and ARB=0 for the conditions that there is no ARB found in a sputum image). Table II shows the results of a comparison between the results of the proposed method and the doctors' evaluation. Based on Table II, Cohen's Kappa Coefficient Value is 0.838. Based on Cohen's Kappa Interpretation Agreement in Table III with Kappa value of 0.838, the proposed method has strong agreement intensity with a manual test performed by the doctors. For the comparison results, the proposed segmentation method is compared to the commonly used methods like  $k$ -means clustering method for color image segmentation [8, 18, 23, 24]. Figure 7 shows the comparison result between the proposed method and  $k$ -means clustering method for color image segmentation. It shows that the proposed method outperforms the  $k$ -means methods. In most of the images, the segmented images using  $k$ -means method contain not only a tiny object like a noise that should be eliminated, but also big result of the failure in identification background. In  $k$ -means method, most of ARB can be grouped as one cluster, but ARB is not separated from the background. In the datasets, ARB color properties have similar color properties of the bright background.

The results of the proposed method are shown in Fig. 8. It highlights that the proposed method can detect most of the ARB with a high level of accuracy. Cohen's Kappa Coefficient Value (0.838) suggests that the proposed method can detect ARBs almost as well as the doctors and as quickly as possible. These results confirm that the proposed method can help reduce the involvement of health personnel in the TB screening

process in the laboratory as a decision support tool.

Although the proposed method successfully detects ARB well, it still has some disadvantages as it has not been able to separate the overlapping ARBs. Overlapping ARB in a sputum image is often detected only as an ARB. It can lead to erroneous ARB counting process. Figure 9 shows that the proposed method is unable to separate overlapping ARBs.

#### IV. CONCLUSION

This research proposes an ARB segmentation method based on Watershed Transformation and Fuzzy C-Means clustering for TB. Watershed Transformation is proven to produce a good candidate area of ARB after the morphological process is previously performed. Furthermore, using Fuzzy C-Means clustering with five classes, the research reveals that the proposed method can detect and quantify the number of ARBs in the image accurately. The test results show the Cohen's Kappa Coefficient value of 0.838. It means that the proposed method can detect the ARB as nearly as good as the doctors. These results confirm the likelihood to use the proposed to help to reduce the involvement of health personnel in the TB screening process in the laboratory as a decision support tool. In the next study, a geometric curve approach will be used to separate overlapping ARBs. It will adopt research by Ref. [25] by using an elliptical curve approach to separate overlapping cervical epithelial cells. Furthermore, this research utilizes four features to differentiate ARB with other available objects on the sputum image. Although it may produce good classification results, the researcher recommended further research to investigate other features to improve the performance of the proposed method such as investigating the use of 80 features in Ref. [26] and 192 features in Refs. [27, 28].

#### ACKNOWLEDGEMENT

The researchers would like to thank The Ministry of Research, Technology, and Higher Education Institution for fully funding this research through the Higher Education Applied Research Grant with contract number 109/SP2H/DRPM/2018.

#### REFERENCES

- [1] World Health Organization. (2018) Global Tuberculosis report 2018. [Online]. Available: [https://www.who.int/tb/publications/global\\_report/en/](https://www.who.int/tb/publications/global_report/en/)
- [2] C. Lambregts van Weezenbeek and J. Veen, "Control of drug-resistant Tuberculosis," *Tubercle and Lung Disease*, vol. 76, no. 5, pp. 455–459, 1995.
- [3] World Health Organization. (2010) Guidelines for treatment of Tuberculosis. [Online]. Available: <https://www.who.int/tb/publications/2010/9789241547833/en/>
- [4] Menteri Kesehatan Republik Indonesia. Keputusan Menteri Kesehatan Republik Indonesia Nomor 364/MENKES/SK/V/2009 tentang pedoman penanggulangan Tuberculosis (TB). [Online]. Available: <https://www.persi.or.id/images/regulasi/kepmenkes/kmk3642009.pdf>
- [5] R. O. Panicker, B. Soman, G. Saini, and J. Rajan, "A review of automatic methods based on image processing techniques for tuberculosis detection from microscopic sputum smear images," *Journal of Medical Systems*, vol. 40, no. 1, p. 17, 2016.
- [6] K. Veropoulos, G. Learmonth, C. Campbell, B. Knight, and J. Simpson, "Automated identification of Tubercle Bacilli in sputum: A preliminary investigation," *Analytical and Quantitative Cytology and Histology*, vol. 21, no. 4, pp. 277–282, 1999.
- [7] M. S. Hossain, F. Ahmed, F. Tuj-Johora, and K. Andersson, "A belief rule based expert system to assess Tuberculosis under uncertainty," *Journal of Medical Systems*, vol. 41, no. 3, pp. 1–11, 2017.
- [8] R. Rulaningtyas, A. B. Suksmono, T. Mengko, and P. Saptawati, "Multi patch approach in  $k$ -means clustering method for color image segmentation in pulmonary Tuberculosis identification," in *2015 4<sup>th</sup> International Conference on Instrumentation, Communications, Information Technology, and Biomedical Engineering (ICICI-BME)*. Bandung, Indonesia: IEEE, Nov. 2–3 2015, pp. 75–78.
- [9] M. Osman, M. Mashor, H. Jaafar, R. Raof, and N. H. Harun, "Performance comparison between RGB and HSI linear stretching for Tuberculosis Bacilli detection in Ziehl-Neelsen tissue slide images," in *2009 IEEE International Conference on Signal and Image Processing Applications*. Kuala Lumpur, Malaysia: IEEE, Nov. 18–19 2009, pp. 357–362.
- [10] M. K. Osman, M. Y. Mashor, and H. Jaafar, "Detection of Mycobacterium Tuberculosis in Ziehl-Neelsen stained tissue images using zernike moments and hybrid multilayered perceptron network," in *2010 IEEE International Conference on Systems, Man and Cybernetics*. Istanbul, Turkey: IEEE, Oct. 10–13 2010, pp. 4049–4055.
- [11] L. Govindan, N. Padmasini, and M. Yacin, "Automated Tuberculosis screening using Zeihl Neelson image," in *2015 IEEE International*

- Conference on Engineering and Technology (ICETECH)*. Coimbatore, India: IEEE, March 20 2015, pp. 1–4.
- [12] M. K. Osman, F. Ahmad, Z. Saad, M. Y. Mashor, and H. Jaafar, "A genetic algorithm-neural network approach for Mycobacterium Tuberculosis detection in Ziehl-Neelsen stained tissue slide images," in *2010 10<sup>th</sup> International Conference on Intelligent Systems Design and Applications*. Cairo, Egypt: IEEE, Nov. 29 – Dec. 1 2010, pp. 1229–1234.
- [13] R. Rulaningtyas, A. B. Suksmono, T. L. Mengko, and P. Saptawati, "Colour segmentation of multi variants Tuberculosis sputum images using self organizing map," *Journal of Physics: Conference Series*, vol. 853, no. 1, pp. 1–6, 2017.
- [14] C. Xu, D. Zhou, T. Guan, and Y. Liu, "A segmentation algorithm for Mycobacterium Tuberculosis images based on automatic-marker watershed transform," in *2014 IEEE International Conference on Robotics and Biomimetics (ROBIO 2014)*. Bali, Indonesia: IEEE, Dec. 5–10 2014, pp. 94–98.
- [15] V. Ayma, R. De Lamare, and B. Castañeda, "An adaptive filtering approach for segmentation of Tuberculosis bacteria in Ziehl-Neelsen sputum stained images," in *2015 Latin America Congress on Computational Intelligence (LA-CCI)*. Curitiba, Brazil: IEEE, Oct. 13–16 2015, pp. 1–5.
- [16] M. K. Osman, M. Y. Mashor, and H. Jaafar, "Segmentation of Tuberculosis Bacilli in Ziehl-Neelsen tissue slide images using hibrid multilayered perceptron network," in *10<sup>th</sup> International Conference on Information Science, Signal Processing and their Applications (ISSPA 2010)*. Kuala Lumpur, Malaysia: IEEE, May 10–13 2010, pp. 365–368.
- [17] P. Soille, *Morphological image analysis: Principles and applications*. Berlin: Springer-Verlag, 1999.
- [18] A. Kurniawardhani, R. Kurniawan, I. Muhimmah, and S. Kusumadewi, "Study of colour model for segmenting Mycobacterium Tuberculosis in sputum images," *IOP Conference Series: Materials Science and Engineering*, vol. 325, no. 1, pp. 1–7, 2018.
- [19] L. Vincent and P. Soille, "Watersheds in digital spaces: An efficient algorithm based on immersion simulations," *IEEE Transactions on Pattern Analysis & Machine Intelligence*, no. 6, pp. 583–598, 1991.
- [20] C. F. F. Costa Filho, P. C. Levy, C. d. M. Xavier, L. B. M. Fujimoto, and M. G. F. Costa, "Automatic identification of Tuberculosis Mycobacterium," *Research on Biomedical Engineering*, vol. 31, no. 1, pp. 33–43, 2015.
- [21] R. Khutlang, S. Krishnan, R. Dendere, A. Whitelaw, K. Veropoulos, G. Learmonth, and T. S. Douglas, "Classification of Mycobacterium Tuberculosis in images of ZN-stained sputum smears," *IEEE Transactions on Information Technology in Biomedicine*, vol. 14, no. 4, pp. 949–957, 2010.
- [22] I. Muhimmah, R. Kurniawan *et al.*, "Automated cervical cell nuclei segmentation using morphological operation and watershed transformation," in *2012 IEEE International Conference on Computational Intelligence and Cybernetics (CyberneticsCom)*. Bali, Indonesia: IEEE, July 12–14 2012, pp. 163–167.
- [23] B. S. Riza, M. Mashor, M. K. Osman, and H. Jaafar, "Automated segmentation procedure for Ziehl-Neelsen stained tissue slide images," in *2017 5th International Conference on Cyber and IT Service Management (CITSM)*. Denpasar, Indonesia: IEEE, Aug. 8–10 2017, pp. 1–5.
- [24] R. Raof, M. Mashor, and S. Noor, "Segmentation of TB Bacilli in Ziehl-Neelsen sputum slide images using *k*-means clustering technique," *CSRID (Computer Science Research and Its Development Journal)*, vol. 9, no. 2, pp. 63–72, 2017.
- [25] I. Muhimmah, R. Kurniawan, and I. Indrayanti, "Overlapping cervical nuclei separation using watershed transformation and elliptical approach in pap smear images," *Journal of ICT Research and Applications*, vol. 11, no. 3, pp. 213–229, 2017.
- [26] J. Chang, P. Arbeláez, N. Switz, C. Reber, A. Tapley, J. L. Davis, A. Cattamanchi, D. Fletcher, and J. Malik, "Automated Tuberculosis diagnosis using fluorescence images from a mobile microscope," in *International Conference on Medical Image Computing and Computer-Assisted Intervention*. Nice, France: Springer, Oct.1–5 2012, pp. 345–352.
- [27] S. Jaeger, A. Karagyris, S. Candemir, L. Folio, J. Siegelman, F. Callaghan, Z. Xue, K. Palaniappan, R. K. Singh, S. Antani, G. Thoma, W. Yi-Xiang, L. Pu-Xuan, and C. J. McDonald, "Automatic Tuberculosis screening using chest radiographs," *IEEE Transactions on Medical Imaging*, vol. 33, no. 2, pp. 233–245, 2014.
- [28] S. Vajda, A. Karagyris, S. Jaeger, K. Santosh, S. Candemir, Z. Xue, S. Antani, and G. Thoma, "Feature selection for automatic Tuberculosis screening in frontal chest radiographs," *Journal of Medical Systems*, vol. 42, no. 8, p. 146, 2018.